Implementation of Sea Ice in the Wave Model SWAN

W. Erick Rogers

Ocean Dynamics and Prediction Branch
Oceanography Division

April 24, 2019

REPORT DOCUMENTATION PAGE

1. REPORT DATE (DD-MM-YYYY)	2. REPORT TYPE	3. DATES COVERED (From - To)
24-04-2019	Memorandum Report	

4. TITLE AND SUBTITLE	5a. CONTRACT NUMBER
Implementation of Sea Ice in the Wave Model SWAN	5b. GRANT NUMBER
	5c. PROGRAM ELEMENT NUMBER 0602435N

6. AUTHOR(S)	5d. PROJECT NUMBER
W. Erick Rogers	5e. TASK NUMBER
	5f. WORK UNIT NUMBER 6A50

7. PERFORMING ORGANIZATION NAME(S) AND ADDRESS(ES)	8. PERFORMING ORGANIZATION REPORT NUMBER
Naval Research Laboratory 1005 Balch Blvd. Stennis Space Center, MS 39529-5004	NRL/MR/7322--19-9874

9. SPONSORING / MONITORING AGENCY NAME(S) AND ADDRESS(ES)	10. SPONSOR / MONITOR'S ACRONYM(S)
Office of Naval Research One Liberty Center 875 North Randolph Street, Suite 1425 Arlington, VA 22203-1995	ONR
	11. SPONSOR / MONITOR'S REPORT NUMBER(S)

12. DISTRIBUTION / AVAILABILITY STATEMENT

DISTRIBUTION STATEMENT A: Approved for public release; distribution unlimited.

13. SUPPLEMENTARY NOTES

14. ABSTRACT

The Naval Research Laboratory has implemented sea ice in SWAN, which is one of the two models used for operational prediction of wind-generated ocean waves by the U.S. Navy. This report describes the methods and implementation. The associated, new user commands are also described. The new code is verified using idealized test cases, and is found to perform as expected. Validation against observational data will be performed and reported separately.

15. SUBJECT TERMS

SWAN	WAVEWATCH III	Wave model
Sea ice	Wave-ice interactions	

16. SECURITY CLASSIFICATION OF:			17. LIMITATION OF ABSTRACT	18. NUMBER OF PAGES	19a. NAME OF RESPONSIBLE PERSON W. Erick Rogers
a. REPORT Unclassified Unlimited	b. ABSTRACT Unclassified Unlimited	c. THIS PAGE Unclassified Unlimited	Unclassified Unlimited	30	19b. TELEPHONE NUMBER (include area code) (228) 688-4727

This page intentionally left blank.

CONTENTS

Listing of figures

Executive Summary

The Naval Research Laboratory has implemented sea ice in SWAN, which is one of the two models used for operational prediction of wind-generated ocean waves by the U.S. Navy. This report describes the methods and implementation. The associated, new user commands are also described. The new code is verified using idealized test cases, and is found to perform as expected. Validation against observational data will be performed and reported separately.

This page intentionally left blank.

1. Introduction

Though it is gradually migrating to use WAVEWATCH III® (WW3, WW3DG 2016) for more and more areas, the U.S. Navy still uses the SWAN model (Booij et al. 1999) for much of its regional wave modeling, because of the efficiency of that model at high resolution and relative ease of use. The operational models include regions that are seasonally ice-infested, such as the Baltic Sea and Gulf of Bothnia, but surprisingly, *there is no representation of sea ice in SWAN.* This obviously can have dire outcome for model accuracy in these regions. With this motivation, we (NRL) have implemented input/output for sea ice in SWAN, a dissipation source term, and scaling of wind input source functions by sea ice. We build on lessons learned during our implementation of sea ice in WW3 (Rogers and Orzech 2013; Rogers et al. 2016). Thus, we have implemented a simple empirical parametric model (polynomial function) for dissipation by sea ice, following Meylan et al. (2014), Collins and Rogers (2017) and Rogers et al. (2018b). Herein, we present verification of this new SWAN code using idealized test cases, to confirm that the model and user controls produce expected results. Validation using realistic test cases is not included in this report. This will be presented in a subsequent manuscript.

2. Background and historical context

2.1. General background

SWAN ('Simulating Waves Nearshore', Booij et al. 1999) belongs to a group called 'third generation wave models' (3GWAMs). These are 'phase-averaged' insofar as they do not represent individual waves, but instead represent waves as spectra. The label of 'third generation' indicates that the models do not make a priori assumptions about spectral shape, distinguishing them from earlier computer models popular in the 1970s and 1980s. Two other 3GWAMs are WAM ('Wave Model', WAMDIG 1988, Komen et al. 1994) and WAVEWATCH III® (WW3) (Tolman 1991, WW3DG 2016).

The dependent variable of WAM is the wave energy spectral density E, and the dependent variable of WW3 and SWAN is the wave action spectral density, $N = E/\sigma$, where σ is the wave frequency, $\sigma = 2\pi/T$ (T denoting wave period). The spectrum is a function of wavenumber or frequency (k or σ), direction (θ), space (x,y), and time (t). The left hand side of the radiative transfer equation includes terms for time rate of change and propagation in the four dimensions (kinematics), while the right hand side includes source functions (dynamics):

$$\frac{\partial N}{\partial t} + \nabla \cdot \vec{c} N = \frac{S}{\sigma} \qquad (1)$$

where $\vec{c}$ is a four-component vector describing the propagation velocities in x, y, k, and θ. For example, in absence of currents, c_x is the x-component of group velocity C_g. The sum of all source functions is denoted as S, and individual source functions are denoted with appropriate subscript, for example dissipation by whitecapping is S_{wc}, and dissipation by ice is S_{ice}. For more detailed description of SWAN, we refer the reader to Booij et al. (1999) and the SWAN technical documentation (SWAN team 2018).

For operational wave modeling, the U.S. Navy uses the WW3 model for coarser resolutions, e.g. 4 km, and the SWAN model for finer resolutions, e.g., 1 km. This choice is based purely on considerations of computational efficiency: SWAN uses an implicit propagation scheme, so that

---

higher resolution does not force small time step sizes (unconditional stability). WW3, on the other hand, uses numerical and parallelization techniques which make it more efficient for larger-scale modeling. At intermediate resolutions, one model or the other may be more efficient, depending on factors such as the number of sea points (workload) and the number of MPI processes used (scaling). In terms of kinematics and dynamics, there is much that the two models have in common. They share the same governing equation (wave action conservation equation) but use different approaches to solving it. The physics parameterizations are roughly comparable between the two models. There are a few phenomena represented in SWAN but not in WW3 (approximated diffraction, and dissipation by vegetation) and a few represented in WW3 but not SWAN (e.g. the various effects of sea ice). In many cases, the same phenomenon is represented in both models, but the options available are different (bottom friction, wind input, whitecapping, nonlinear interactions, etc.). The numerical and grid approaches in the two models differ significantly. SWAN uses implicit geographic propagation schemes while WW3 uses explicit schemes (excepting the case of unstructured grids). SWAN solves propagation and source terms together, while WW3 uses split time stepping. WW3 permits two-way nesting; SWAN does not. WW3 treats unresolved islands using obstruction grids, while SWAN includes simple obstacles such as breakwaters using simple geometries. WW3 allows masking of portions of the domain; SWAN does not.

2.2. Sea ice in wave models

In version 1 of WW3 (Tolman 1997), the model was already designed such that ice concentration could be ingested, and if the concentration exceeded some threshold (e.g. 50%), the grid cell was deactivated (treated as land). Below the threshold, the grid cell was treated as open water. Early treatment of ice in WAM is not well-documented. Komen et al. (1994) mention treatment of the central ice pack as land, but there is no indication that the model actually ingested ice. Rather, the behavior was most likely produced by pre-processing of the bathymetry or a land/sea mask. This was the approach taken by Tuomi et al. (2011) in their application of WAM for the Baltic Sea.

In WW3 version 2 (Tolman 2002), the Tolman (2003) scheme was implemented, which optionally instructs the model to use partial transmission for intermediate ice coverage (e.g. 25% to 75%). This scheme was known as the "continuous treatment" of sea ice. With version 4 of WW3 (Tolman et al. 2014), this "continuous treatment" of sea ice was given the designation "IC0", to distinguish it from the other options (IC1, IC2, IC3) which appeared for the first time in that version. The latter options were implemented as physics parameterizations on the right-hand side of the governing equation: S_{ice}. The first S_{ice} parameterizations were implemented in ECWAM (the European Centre's version of WAM, see glossary) and WW3 at roughly the same time: Doble and Bidlot (2013) and Rogers and Orzech (2013), respectively. The concept of such a source term was not new, e.g. Komen et al. (1994).

Descriptions of source terms for dissipation of wave energy by sea ice in WW3 can be found in Rogers et al. (2018a) and WW3DG (2016). In this document, we are only concerned with the method denoted as "IC4" in WW3. We utilize the same notation for our implementation in SWAN. The "IC4" S_{ice} is a set of simple empirical/parametric source term options, where "Method 1", "Method 2", etc. are denoted as IC4M1, IC4M2, etc. IC4 was first introduced in Collins and Rogers (2017), with an additional option (IC4M7) added by Rogers et al. (2018a).

The seven methods are summarized in Rogers et al. (2018a). IC4M2 is a prescription of the dissipation rate as a polynomial dependent on wave frequency. This is the method that is implemented in SWAN here, and it is described in detail in Section 3.3.2. IC4M6 is a prescription of the dissipation rate as a step function dependent on wave frequency. This method has been used extensively by NRL in WW3 hindcasts. New suggestions for how to use IC4M2 and IC4M6 are found in Rogers et al. (2018a,b).

2.3. Sea ice in SWAN

SWAN, during the 2000s, was positioned as a model that could be widely used by both researchers and engineers. In the research role, it was gradually expanded to have many different options for physics parameterizations, kinematics and numerics. This followed a relatively open policy, that if a feature could be coded and published in a peer-reviewed paper, then it should be provided for other scientists to use and experiment with. Practical matters, such as suitability for particular applications, or suitability for routine use, were left to the user to decide. Some of the phenomena targeted are expected to have a limited user-base: for example, diffraction, triads, dissipation by mud, and dissipation by vegetation[1]. Thus, it is perhaps surprising that at time of writing (2019), there is still no implementation of something as obvious as sea ice in the public release version of SWAN.

This absence did not, however, mean that SWAN users modeling ice-infested waters had no way to deal with it. As with WAM, a user could develop a pre-processing system to automatically modify the land/sea boundaries (using input bathymetry or water levels) based on sea ice concentration thresholds. We know of one definite example of this. In 2011, such a scheme was implemented for use within the ADCIRC/SWAN coupled modeling system. This was reported in slides for an ADCIRC workshop (Asher 2012). This was done for storm surge modeling in Lake Erie in winter, where there exist competing effects which determine wave conditions: relatively strong winds from winter storms and partial ice cover, which often reduces fetch. The changes to the SWAN code itself are minimal (just a few lines), and have no functionality outside the ADCIRC/SWAN system. Most of the associated code is within the coupler. Ice is provided by ADCIRC to the coupler, which modifies the depths and provides them to SWAN. The user command to activate the method in SWAN is 'CICE'. In the present work, we do not use this command, because for many people, it would incorrectly imply association with the well-known sea ice model of the same name (see glossary).

3. Implementation

3.1. Strategy

Our strategy is to provide a *complete* implementation of a relatively *simple* approach and provide that for review by SWAN code administrators (Delft U.) and subsequent public release. In a follow-up effort, more complex approaches can be implemented, using the foundation provided by the initial method. The word '*complete'* here refers to all of the necessary input/output (i/o), functionality, user-interface, and documentation. We anticipate that much of the i/o can be applied for more complex methods in the future. The word '*simple'* here refers to the source

---

[1] In the case of diffraction and triads, many users will prefer to use a phase-resolving model rather than SWAN. In the case of dissipation by mud and vegetation, it is a severe challenge to adequately describe the input fields.

function itself. We use a parametric form that can be controlled using a brief list of instructions. This is in contrast to 1) a more complex method, such as a viscoelastic model or boundary layer approximation which may require complex solution procedures or look-up tables, or 2) a method that is simple in concept but requires a longer sequence of user instructions (e.g. the IC4M6 step function). Also, in this initial version, we do not address phenomena such as scattering and reflection by ice, or the effect that ice has on kinematics (i.e. refraction and shoaling by ice) which remains as a largely academic problem in the context of WW3. The word '*simple*' does *not* apply to the code changes for this first version. In particular, substantial changes to the model i/o were required.

The parametric/empirical approach adopted is a pragmatic approach, with the primary question of 'What can be easily applied in an operational context?' and the secondary question of 'What is the simplest code that gives the desired model behavior?'. The main feature of the desired behavior was a flexible (user-defined) functional dependence of dissipation rate on frequency, with spatially and varying ice concentration fields.

With these relatively constrained objectives, the work reported here (code development and design of idealized cases) was completed by one person (the author) in a relatively short time, working intermittently during late December 2018 to early February 2019. The work also benefitted from lessons learned during the WW3 implementation: with the benefit of hindsight, one can very clearly identify tasks during the WW3 implementation where time invested yielded larger returns.

3.2. Model version and version control

Here, the sea ice implementation was created starting from the *public release* version of SWAN. That is version 41.20AB, which is the most recent version circa December 2018-February 2019. Here, 'A' and 'B' refer to patches, with patch A dated May 3 2018 and patch B dated November 30 2018. The SWAN v41.20AB user manual is therefore referenced here as 'SWAN team (2018)'. The new version with sea ice is denoted as '41.20ABi' within the code itself. This version was provided to the SWAN code administrators (Delft U.) February 6 2019.

Notably, the starting point was *not* the NRL version of SWAN which is used operationally by the U.S. Navy. In order for the new sea ice feature to be available for Navy operations, the new code must be ported to the NRL version. This porting is not completed at time of writing.

The new SWAN code, 41.20ABi, was developed on a Subversion (SVN) repository provided by Prof. Nirnimesh Kumar of the U. Washington.

The selection of the latest Delft public release version (41.20AB) over the NRL version as the 'base' for the new SWAN-ice code had/has the following advantages:
1) It is expected to facilitate incorporation of the NRL code changes into a future public release.
2) It allowed our external collaborator, Dr. Kumar, to receive our code changes rapidly. UW does not have access to the NRL repository. At time of writing, Dr. Kumar has begun work on realistic applications of the 41.20ABi code developed by NRL.

3.3. Methods

Sea ice has two effects in this implementation. The first is a direct dissipation of wave energy. The second is a reduction of wind input. Both effects are controlled by user settings. These are described in this section, along with a brief description of the input/output features.

3.3.1. Input

Primary input is in the form of ice concentration as a fraction (Section 3.4.1). This is denoted as a_{ice} and is between 0.0 and 1.0. The variable may be nonstationary and/or non-uniform, much like existing fields such as wind vectors, currents, and water levels. The user is also allowed the option of specifying a constant and uniform ice concentration (Section 3.4.2). The latter exists primarily for idealized scenarios and simple testing.

Secondary input is ice thickness in meters. However, at time of writing, no source term uses this ice thickness. It is therefore undocumented in 41.20ABi. It exists only as a feature to be exploited by a future ice source term.

3.3.2. Ice source term

Using the command 'IC4M2', the user activates a source term S_{ice} to represent the dissipation of wave energy by sea ice. The IC4M2 method is empirical/parametric: S_{ice} is a polynomial based on wave frequency. The user provides the coefficients for the polynomial.

The name 'IC4M2' comes from Collins and Rogers (2017), where the same method is implemented in the WAVEWATCH III model (WW3DG 2016), though the notation is changed here. That method, in turn is a generalization of the formula proposed by Meylan et al. (2014).

Following the notation of Rogers and Orzech (2013), the temporal exponential decay rate of energy can be written as:

$$D_{ice} = \frac{S_{ice}}{E} = -C_g \alpha = -2C_g k_i$$

where S_{ice} is the new source term, and E is the wave energy spectrum. Here, k_i is the linear exponential attenuation rate of wave amplitude in space, $a(x) = a_0 \exp(-k_i x)$. The factor 2 here provides a conversion from amplitude decay to energy decay: $\alpha = 2k_i$. The C_g provides conversion from spatial decay to temporal decay. S_{ice} and E vary with frequency and direction: $S_{ice}(f, \theta), E(f, \theta)$. In the case of IC4M2, D_{ice} and k_i may vary with frequency, according to user settings, but not direction: $D_{ice}(f), k_i(f)$.

The ice source function is scaled with ice concentration:

$$S_{ice,2} = a_{ice} S_{ice,1}$$

where 1 denotes the value before scaling and 2 denotes the value after scaling.

For S_{ice} method IC4M2,

$$k_i = C_0 f^0 + C_1 f^1 + \cdots + C_6 f^6$$

Here, k_i has units of 1/m , f has units of Hz, and so C0, C1, etc. are dimensional, e.g. C2 has units of $s^2 m^{-1}$.

WW3DG (2016) and Collins and Rogers (2017) implement a functionally equivalent formula,

$$\alpha = C_{1,ww}f^0 + C_{2,ww}f^1 + \cdots + C_{5,ww}f^4$$

Thus, anyone using IC4M2 in both models should be aware of three differences: 1) there is different numbering of coefficients, 2) there is a different number of terms, and 3) WW3 formula is in terms of α, while ours is in terms of k_i (factor two difference).

We provide two example applications:
1) SWAN: [C_2=1.06e-3 , C_4=2.30e-2] or WW3: [$C_{3,ww}$=2.12e-3 , $C_{5,ww}$=4.59e-2]. This recovers the polynomial of Meylan et al. (2014). The Meylan case is for ice floes, mostly 10 to 25 m in diameter, in the marginal ice zone near Antarctica.
2) SWAN: [C_2=0.284e-3 , C_4=1.53e-2] or WW3: [$C_{3,ww}$=0.568e-3 , $C_{5,ww}$=3.06e-2]. This recovers the 'WA3 UK' polynomial of Rogers et al. (2018b). This is for a case of pancake and frazil ice, where both coefficients are, of course, smaller than the first example.

Given the three differences between the SWAN and WW3 methods of inputting the coefficients, it is worthwhile to confirm that the $k_i(f)$ profiles from the two models for the two examples are indeed equivalent. This is done in Figure 1. There is, of course, difference in the frequency ranges of the two models: WW3 typically has a maximum prognostic frequency of 0.40 to 0.75 Hz, while SWAN typically includes a larger range, e.g. to 1.0 Hz. In the figure, Meylan et al. (2014) is denoted as 'M14'.
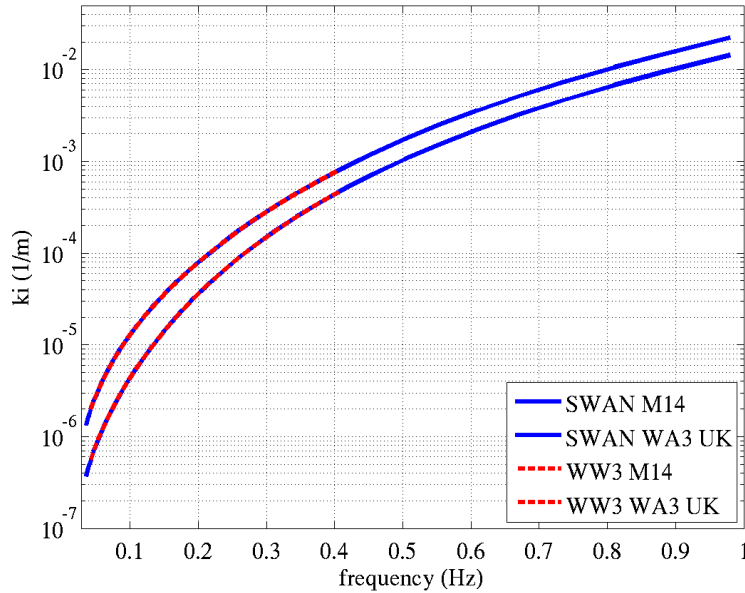

Figure 1. Confirmation that the two methods of inputting a polynomial in SWAN (using C_2 and C_4) and WW3 (using $C_{3,ww}$ and $C_{5,ww}$) are equivalent. See text for values used.

3.3.3. Impact on wind input source functions

The effect on wind input is a scaling of the wind input source functions by open water fraction. The user may disable or reduce this effect.

The variable Ω_{iw} controls the scaling of wind input by open water fraction. It is denoted in the code as 'ICEWIND'. The default value is $\Omega_{iw} = 0$. This corresponds to the case where wind input is scaled by the open water fraction.

The relevant formula is a simple factor F_{in} applied to the wind input source function S_{in}:
$$F_{in} = (1 - a_{ice}(1 - \Omega_{iw}))$$
This can be re-written as :
$$F_{in} = a_{water} + a_{ice}\Omega_{iw}$$
where a_{water} is open water fraction and $a_{water} + a_{ice} \equiv 1.0$.

Thus, in terms of the action balance equation, the scaling is
$$\frac{\partial N}{\partial t} + \nabla \cdot \vec{c}N = F_{in}\frac{S_{in}}{\sigma} + \frac{S_{nl4}}{\sigma} + \frac{S_{wc}}{\sigma} + \frac{S_{bf}}{\sigma} + a_{ice}\frac{S_{ice}}{\sigma} + \frac{S_{etc.}}{\sigma}$$
and with the default scaling, $\Omega_{iw} = 0$, it is
$$\frac{\partial N}{\partial t} + \nabla \cdot \vec{c}N = (1 - a_{ice})\frac{S_{in}}{\sigma} + \frac{S_{nl4}}{\sigma} + \frac{S_{wc}}{\sigma} + \frac{S_{bf}}{\sigma} + a_{ice}\frac{S_{ice}}{\sigma} + \frac{S_{etc.}}{\sigma}$$
Here, we use $S_{nl4}, S_{wc}, S_{bf}, S_{etc.}$ to indicate four-wave nonlinear interactions, dissipation by whitecapping, dissipation by bottom friction, and other source terms, respectively. These source terms are not scaled.

The impact of sea ice on "source terms" in the real ocean, including S_{in}, is not known with any certainty, and instead is primarily based on intuition and guesswork: see discussion in Rogers et al. (2016).

Our own visual observations during one particular case of an ice-covered ocean during moderate-to-high winds, e.g. U_{10}=15 m/s indicated that whitecapping within ice cover is essentially zero. (Here we are referring to the 'Sea State Wave Array 3' case depicted in Figure 1 of Rogers et al. (2016).) In the context of practical applications with the threshold-based whitecapping dissipation S_{ds}, available as 'ST6' in SWAN (Rogers et al. 2012), we expect that S_{ds} within the ice cover will often be zero, as it would fall under the breaking threshold as a result of the action of S_{ice}. In that case, the question of scaling becomes moot.

Since the exponential wind input occurs through the action of normal stresses, there is no obvious reason for wind input to be disabled in case of a pliable ice cover. For example, if the wavelength is 100 m, and the ice floe diameters are 1 m, that normal stress should not be affected. However, for the reverse case, say wavelength of 20 m and rigid floes of 100 m or more, then of course the normal stress would be affected. This thought experiment suggests the possibility of using the floe size to determine the scaling. Lastly, we must also mention the calming effect that oil is sometimes alleged to have on waves. For those who accept this as fact, it may be easier to believe in full suppression of wind input by ice cover, regardless of floe size.

The F_{in} factor was apply to all wind input source functions in SWAN. These include:
- the wind input source function for 1st- and 2nd- generation mode of running SWAN
- linear wind input according to Cavaleri and Malanotte-Rizzoli (1981) and Tolman (1992)
- exponential wind input from Snyder et al. (1981) and Komen et al. (1984)
- exponential wind input from Janssen (1989, 1991)

- exponential wind input from Yan (van der Westhuysen et al. 2007)
- linear and exponential wind input for ST6 (Donelan et al. 2006, Tsagareli et al. 2010, Rogers et al. 2012)

3.3.4. Output

The re-gridded and/or interpolated ice concentration field $a_{ice}(\vec{x}, t)$ is available as an output, in the same fashion as wind and water level are available as output fields. Here, $\vec{x}$ indicates geographic location and t indicates time.

As noted in Section 3.3.2, S_{ice} varies in frequency and direction, $S_{ice}(f, \theta)$. From this, two reduced variables can be computed:

$$S_{ice,1d}(f) = \int S_{ice}(f, \theta)d\theta$$

$$S_{ice,0d} = \iint S_{ice}(f, \theta)df d\theta = \int S_{ice,1d}(f)df$$

The integrated (bulk) parameter $S_{ice,0d}$ can be output as $S_{ice,0d}(\vec{x}, t)$. This is denoted as 'DISICE' and is analogous to existing output options such as 'DISBOT' for integrated bottom friction. In addition to block output, a_{ice} and $S_{ice,0d}$ can be included in table output.

At 'test points', the spectral parameters $S_{ice,1d}(f)$ and $S_{ice}(f, \theta)$ can be provided as output. Again, this is analogous to existing features for obtaining output for other source terms, such as bottom friction.

3.3.5. Summary of implementation
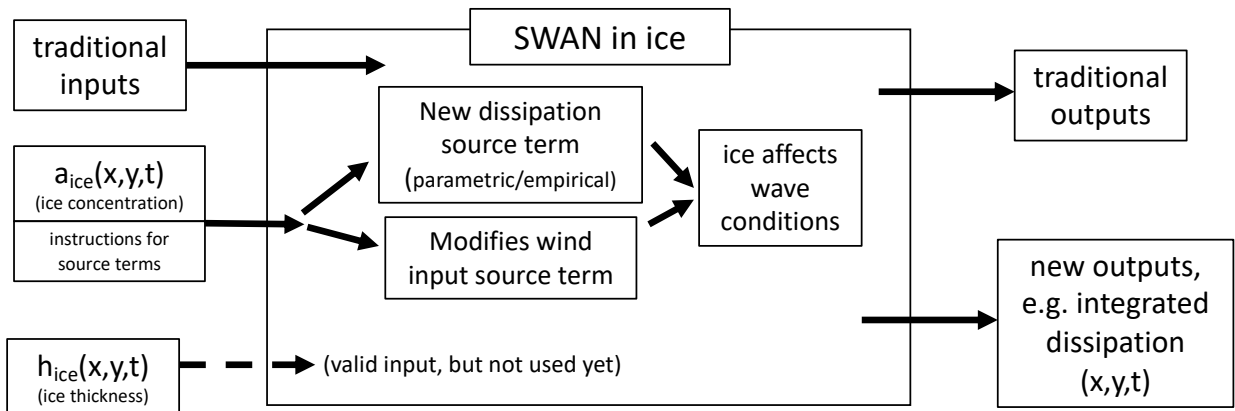
The implementation is summarized in Figure 2.

Figure 2. Simple schematic summarizing the ice-related changes to SWAN.

3.4. User interface

3.4.1. Input fields

The ice concentration a_{ice} is a new input field, denoted as 'AICE'. It is added to the 'INPgrid' and 'READinp' commands as follows:

```
!   INPgrid
!      BOTtom / WLEVel / CURrent / VX / VY / FRiction / WInd / WX / WY
!      NPLAnts / TURB / MUDL / AICE
!      | REG [xpinp] [ypinp] [alpinp]  [mxinp] [myinp]  [dxinp] [dyinp] |
!    <  CURVilinear [stagrx] [stagry] [mxinp] [myinp]                   >
!      | UNSTRUCtured                                                   |
!      (NONSTATionary [tbeginp] [deltinp] SEC/MIN/HR/DAY [tendinp])


!   READinp    BOTtom/WLevel/CURrent/FRiction/WInd/COORdinates/
!              NPLAnts/TURB/MUDL/AICE
!         [fac]  / 'fname1'         \
!                  \ SERIES 'fname2' /  [idla] [nhedf] ([nhedt]) (nhedvec))
!         FREE / FORMAT 'form' / [idfm] / UNFORMATTED
```

The above is intended documentation for the next public release. Ice thickness h_{ice} is included in the code as 'HICE' but is intentionally not documented.

3.4.2. Instructions for new source term

The instructions for the IC4M2 form of S_{ice} are as follows:

```
!   IC4M2 [AICE] [C0] [C1] [C2] [C3] [C4] [C5] [C6]
```

Here, the 'AICE' is an optional field to specify a_{ice} as stationary and uniform. This is for use in idealized test cases and is similar to using the existing 'WIND' command in SWAN to specify stationary and uniform wind. If ice concentration is provide by the user as nonstationary and/or nonuniform via INPgrid and READinp, then the 'AICE' field here is ignored.

An example in Section 3.3.2 has [C_2=1.06e-3, C_4=2.30e-2], following Meylan et al. (2014) (broken floes). The user command for this would be:

```
IC4M2 1.0 0.0 0.0 1.06e-3  0.0 2.30e-2 0.0  0.0
```

The second example from Section 3.3.2 has [C_2=0.284e-3, C_4=1.53e-2], from Rogers et al. (2018b) (pancake and frazil ice). The user command would be :

```
IC4M2 1.0 0.0 0.0 0.284e-3 0.0 1.53e-2 0.0  0.0
```

3.4.3. Instructions for modification of wind input source functions

The parameter Ω_{iw} described in Section 3.3.3 is defined using the 'SET' command:

```
!   SET  [level]  [nor]  [depmin]  [maxmes]                &
!        [maxerr]  [grav]  [rho] [cdcap] [uscap] [inrhog]  &
!        [hsrerr] CARTesian/NAUTical  [pwtail]             &
!        [froudmax] [sort]  [nsweep]  [icewind] CURV       &
!        [printf]  [prtest] (not documented)
```

Three examples follow:
```
1) SET ICEWIND 0.0
```
→ Here, wind input is scaled by the open water fraction. This is the default.

9

```
2) SET ICEWIND 1.0
```
→ Here, ice does not affect wind input directly. Note that the indirect effect via S_{ice} may still be large, and can in fact fully suppress wind input.

```
3) SET ICEWIND 0.5
```
→ This indicates partial scaling.

3.4.4. Output

Ice concentration (a_{ice} or 'AICE') and spectral-integrated dissipation by sea ice ($S_{ice,0d}$ or 'DISICE') can be requested as 'BLOCK' or 'TABLE' output as follows:

```
!    ------------------------------------------------------------------
!    BLOCK   'sname'  HEADER / NOHEADER  'fname' (LAY-OUT [idla])
!            < DSPR/HSIGN/DIR/PDIR/TDIR/TM01/RTM01/RTP/TM02/FSPR/DEPTH/VEL/
!              FRCOEFF/WIND/DISSIP/QB/TRANSP/FORCE/UBOT/URMS/WLEN/STEEPNESS/
!              DHSIGN/DRTM01/LEAK/TSEC/XP/YP/DIST/SETUP/TMM10/RTMM10/
!              TMBOT/QP/BFI/WATLEV/BOTLEV/TPS/DISBOT/DISSURF/DISWCAP/
!              GENE/GENW/REDI/REDQ/REDT/PROPA/PROPX/PROPT/PROPS/RADS|LWAVP/
!              DISTUR/TURB/DISSWELL/AICE/DISICE
!              PTHSIGN/PTRTP/PTWLEN/PTDIR/PTDSPR/PTWFRAC/PTSTEEPNESS>
!              ([unit]) (OUTPUT [tbegblk] [deltblk] SEC/MIN/HR/DAY)
!    ------------------------------------------------------------------


!    ------------------------------------------------------------------
!    TABLE   'sname'  HEADER / NOHEADER / INDEXED 'fname'
!            < DSPR/HSIGN/DIR/PDIR/TDIR/TM01/RTM01/RTP/TM02/FSPR/DEPTH/VEL/
!              FRCOEFF/WIND/DISSIP/QB/TRANSP/FORCE/UBOT/URMS/WLEN/STEEPNESS/
!              DHSIGN/DRTM01/LEAK/TIME/TSEC/XP/YP/DIST/SETUP/TMM10/RTMM10/
!              TMBOT/QP/BFI/WATLEV/BOTLEV/TPS/DISBOT/DISSURF/DISWCAP/
!              GENE/GENW/REDI/REDQ/REDT/PROPA/PROPX/PROPT/PROPS/RADS|LWAVP/
!              DISTUR/TURB/DISSWELL/AICE/DISICE
!              PTHSIGN/PTRTP/PTWLEN/PTDIR/PTDSPR/PTWFRAC/PTSTEEPNESS>
!              ([unit]) (OUTPUT [tbegtbl] [delttbl] SEC/MIN/HR/DAY)
!    ------------------------------------------------------------------
```

Ice concentration is expressed as a fraction. This is a user input variable, and with BLOCK and TABLE, it is interpolated by SWAN as requested by the user, similar to the way that the user can request the wind vector as an output from SWAN. DISICE is analogous to similar outputs DISBOT, DISSWCAP, etc.

3.5. Brief list of components

Below is a list of the 10 most significant changes to the code.
1) Addition of 'AICE' and 'HICE' to gridded input variables via 'INPgrid' and 'READinp'.
2) Addition of 'ICEWIND' to 'SET' command.
3) Addition of 'IC4M2' command.
4) Addition of 'AICE/HICE/DISICE' to 'BLOCK/TABLE' output.
5) Addition of 0-d (scalar/bulk), 1-d (frequency-dependent), and 2-d (frequency/direction-dependent) output of S_{ice} to 'TEST' output.
6) Creation of new arrays for 'AICE' and 'HICE'. Arrays of each variable exist for both for input grids and computational grids. Latter is a subset of multi-functional 'COMPDA'

array.

7) Creation of output array 'DISICE' (integrated S_{ice} on computational grid). This is a subset of multi-functional 'COMPDA' array.
8) Addition of new subroutine 'SICE' for computations of S_{ice}.
9) Modification of six wind input routines to scale wind input by open water fraction.
10) Where a separate routine is used for the case of unstructured grids, functionality is added. An example is routine 'SwanCompUnstruc' which fills the same role as routine 'SWOMPU' used in structured grid case.

4. Idealized tests

4.1. Simple decay profiles

The most basic test of the new source term is confirmation of empirical decay. This follows similar checks by Rogers and Orzech (2013) and Section 3.2.2 in Rogers et al. (2018a). analytical solution is used as ground truth, simply:

$$H(x) = H_0 e^{-k_i x}$$

which follows from

$$\eta(x, t) = \text{Re}[0.5 H(x) e^{i(kx - \sigma t)}]$$

where Re[] denotes real component, H is waveheight, and $\eta(x, t)$ is the free surface.

In this case, wave conditions are specified at the up-wave boundary.

The following settings are used:
- Deep water
- One-dimensional (i.e. uniform in y)
- Significant wave height at boundary is 1.0 m. Other values were tested, but no difference in normalized wave height was observed (problem is linear).
- Peak period is 10 sec. A case was tested with 14.1 s, which changes the Courant number, but no difference was noted.
- Time step size of 10 minutes was used. A 30 sec time step was also tested, which changes the Courant number, but no difference was noted.
- Source terms other than S_{ice} are inactive.
- Model duration is 1 day. (A 10-second wave would travel the 50 km in 1.8 hours.)
- First order propagation used unless otherwise noted.

Results with 5 km resolution are shown in Figure 3. This figure can be compared directly with Figure 47 of Rogers et al (2018a), in which the same comparison is made using WW3. This result indicates that numerical error is significant with this resolution for cases of $k_i \geq 1 \times 10^{-4}$. This behavior is normal: numerical models are generally poor at representing large changes occurring within a few grid cells. We can also note that while this problem exists in both WW3

and SWAN, the 5 km resolution here is relatively coarse for SWAN. Wave modeling at this resolution can be more efficiently performed using WW3 instead of SWAN.
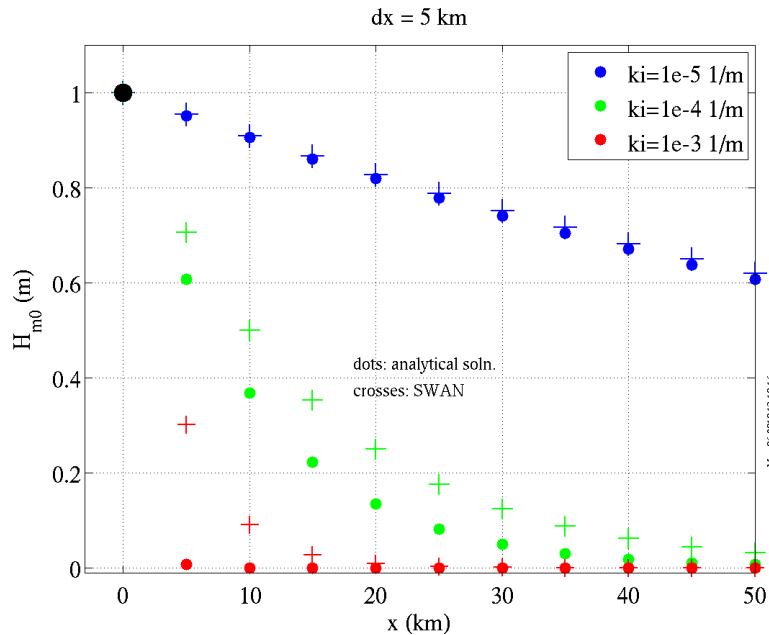

Figure 3. Comparison of coarse-grid SWAN against analytical model for exponential decay. Significant waveheight H_{m0} vs. distance is shown for different k_i values as indicated in legend. Spatial resolution is 5 km. The first order propagation scheme is used.

Results with 1 km resolution, which is a resolution at which SWAN would be more typically applied, are shown in Figure 4. The numerical error is significantly reduced by using higher resolution.

A test was also performed using the higher order propagation scheme (Rogers et al. 2002) which is the default scheme in SWAN. Results are shown in Figure 5 and Figure 6. Results are improved with the higher order propagation scheme. In Figure 6, the first order propagation scheme is denoted as 'BSBT' and the higher order scheme as 'STEL' (see glossary). It may seem counter-intuitive that the numerical scheme affects the outcome, while Courant number does not, since numerical diffusion and dispersion are generally determined by numerical scheme, resolution, and Courant number. However, this test case is in steady state, which affects dependency on time step size.
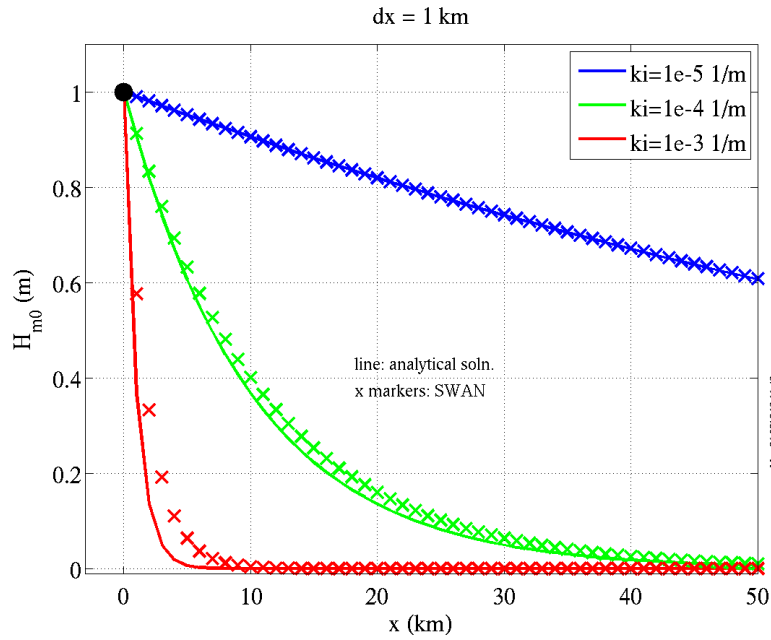
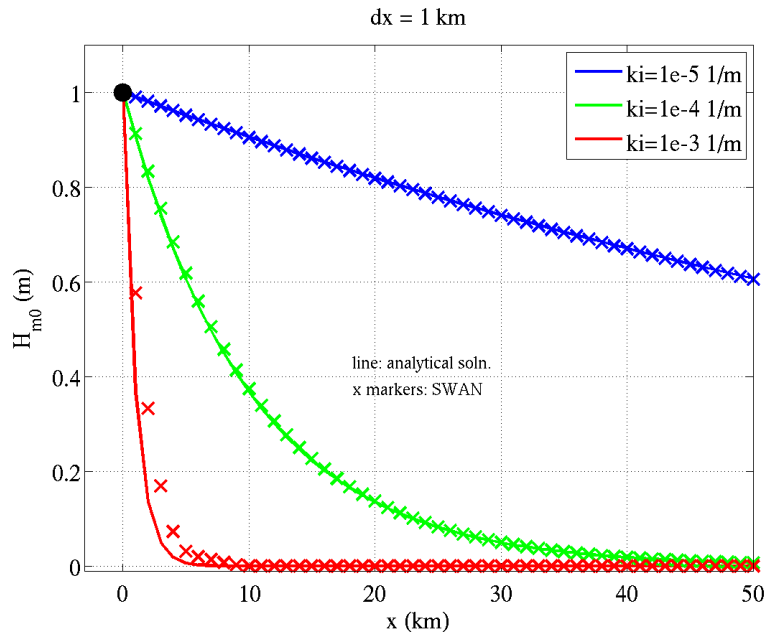Figure 4. Like Figure 3, but fine-grid SWAN: spatial resolution is 1 km.

Figure 5. Like Figure 4, but using the default (higher order) propagation scheme.
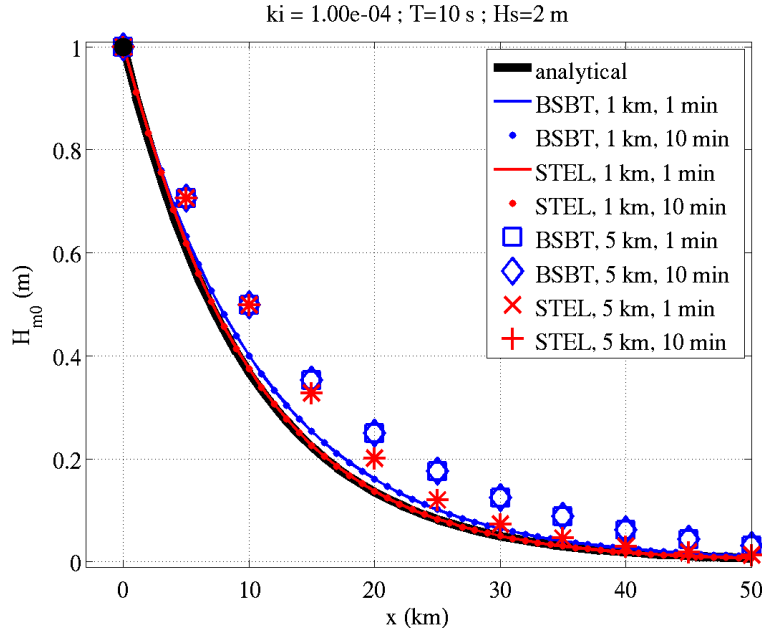
13

Figure 6. Like Figure 3, but showing a single dissipation rate, k_i =1e-4 m^{-1} , with different settings for propagation scheme ('BSBT' vs. 'STEL'), resolution (1 km vs. 5 km), and time step size (1 minute vs. 10 minute), as indicated in legend.

4.2. Swell propagation of nonstationary and non-uniform ice

Next, we look at an idealized test case with nonstationary and non-uniform ice. The primary purpose of the test is to demonstrate the model's ability to read in the nonstationary and non-uniform ice and behave in an expected manner.

Settings are as follows:
- Deep water
- Resolution is 2 km.
- Two-dimensional domain
- Waves travel from left (low-x) to right, forced using swell condition at the left boundary: significant wave height H_s=2.5 m and peak period T_p=14.1 s.
- Time step size of 10 minutes was used.
- Source terms other than S_{ice} are disabled.
- IC4 is used with the 'M14' settings.
- First order propagation scheme is used.
- The model starts 0000 UTC, with no ice.
- Initial condition is in steady state (initialized with stationary computation).
- Ice appears at 0300 UTC, in a subset of the domain as shown in Figure 7.
- H_s reaches new steady state quickly: at 0400-0500 UTC.
- Spectra are saved at two points, indicated in Figure 7: 'Point 1' at x =10 km and 'Point 2' at x =90 km.
- $E(f)$ at Point 2 reaches new steady state at 0600 UTC. During 0400-0600, changes are occurring in the spectral tail (because these are the slowest waves), so $E(f)$ is visibly changing, while H_s changes are small.

14

- Ice disappears at 1500 UTC, and the model proceeds to recover the to the initial (ice-free) state after a few hours.

The result for 1400 UTC is shown in Figure 7. Spectra at two points are shown in Figure 8, also at 1400 UTC. The spectrum at Point 1 is essentially the spectrum of the boundary forcing. The spectrum at Point 2 indicates the impact of S_{ice}. Because the M14 S_{ice} is used, there is much stronger damping of higher frequencies. All results from this test case are what we expect.
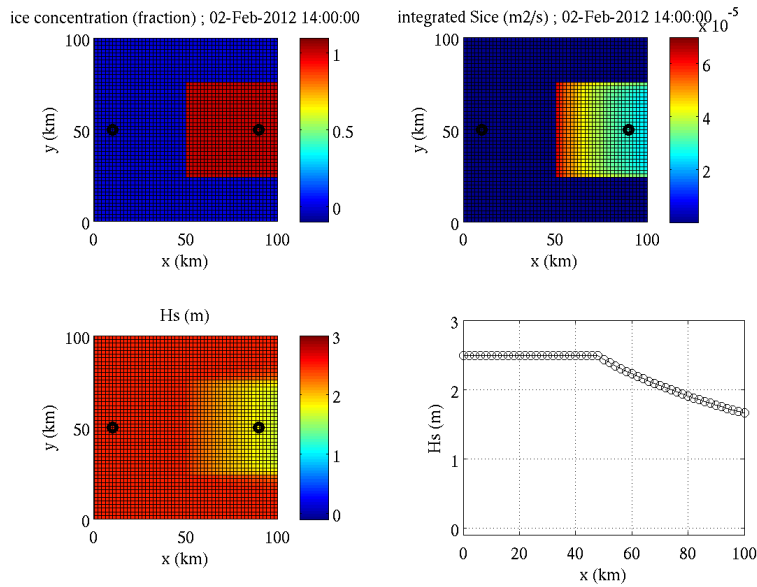

Figure 7. Two-dimensional idealized case with swell prescribed at low-x boundary. Top left: ice concentration. Top right: integrated ice dissipation, $S_{ice,0d}$. Lower left: significant waveheight. Lower right: significant waveheight along a transect at y=50 km. The black circles indicate Point 1 (x=10 km) and Point 2 (at x=90 km). The points are referenced in Figure 8.
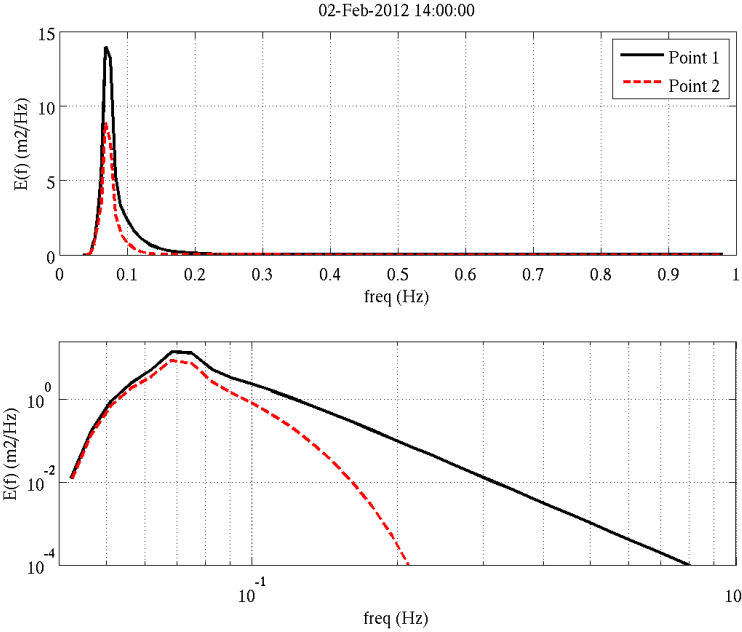
Figure 8. Energy spectra at the two points indicated in Figure 7. Top: *E(f)* on linear scale.
Bottom: *E(f)* on log scale.

4.3. Cases with wind and ice

In this section, we present an idealized test case with winds. Settings are as follows:

- Deep water.
- Resolution is 2 km.
- Two-dimensional domain.
- Wind speed is U_{10}=12 m/s. Wind direction is from right (high-x) to left.
- Closed boundaries (no swell).
- Ice is stationary and non-uniform: Ice covers right (high-x) half of domain.
- Time step size of 10 minutes.
- 1 day duration (results are shown for end of simulation).
- Initial condition (hour zero) is in steady state (initialized with stationary computation).
- ST6 physics parameterization for wind input and whitecapping.
- First order propagation scheme is used.
- IC4 is used with the 'M14' settings.
- Source term output is saved at x=88 km, y=52 km.

Here, we present four ways of running the same test case. The strategy is to show one recommended treatment and three non-standard treatments. The purpose of the latter three is to verify that user-controls are working, rather than to produce results that could be considered "realistic". The four cases and associated figures are as follows:

1) $\Omega_{iw} = 0$ (default) and S_{ice} enabled: Figure 9.
2) $\Omega_{iw} = 0$ (default) and S_{ice} disabled: Figure 10.
3) $\Omega_{iw} = 1$ and S_{ice} enabled: Figure 11, Figure 12.
4) $\Omega_{iw} = 1$ and S_{ice} disabled: Figure 13.

16

The first example, in Figure 9 shows results that are fairly intuitive: growth is fully suppressed within the ice cover. The only energy within the ice cover is tiny, and is associated with swell energy traveling in the $+x$ (backwards) direction, associated with four-wave nonlinear interactions.

The second example, in Figure 10, is like the first, except showing $S_{ice}=0$. The results are not significantly different from the first, because windsea is not generated in the ice either way. However, this second (and rather unrealistic) example illustrates how the impact of ice on S_{in} can be at least as important as the S_{ice} term within the model.
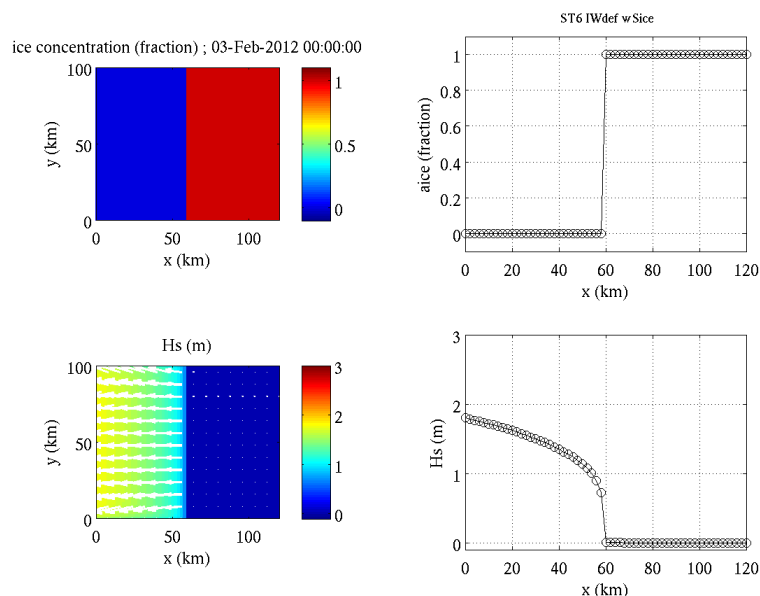

Figure 9. Test case with wind and ice. Top left: ice concentration in 2-d. Top right: ice concentration along a transect at y=50 km. Lower left: significant waveheight in 2-d. Wave direction is indicated with arrows. Lower right: significant waveheight along a transect at y=50 km. In this case, the default treatment of wind input is used (default 'ICEWIND') and S_{ice} is active.
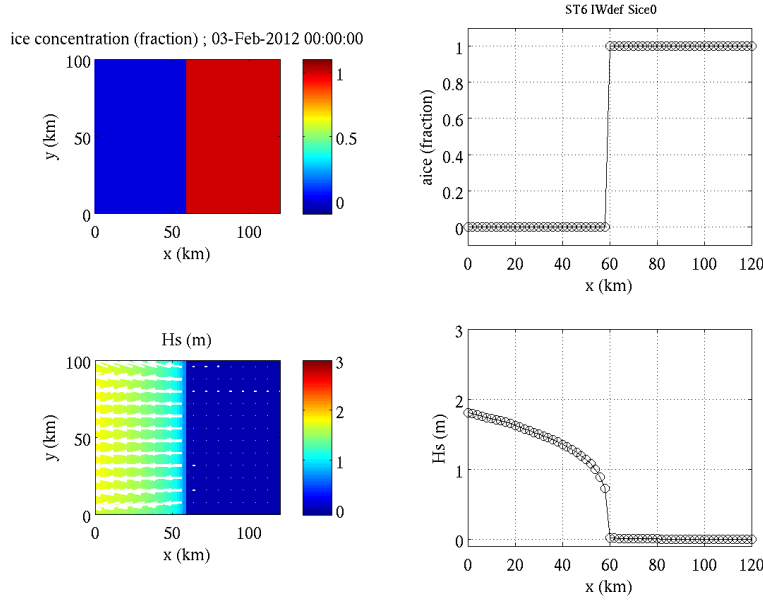
Figure 10. Like Figure 9, except S_{ice}=0.

The case shown in Figure 11 ($\Omega_{iw} = 1$ and S_{ice} enabled) indicates growth of waves within the ice cover. Essentially, the action of the wind input, which is not suppressed at all since $\Omega_{iw} = 1$, overcomes the dissipation by sea ice, S_{ice}. The growth becomes noticeable at a fetch of around 32 km into the domain: this is where there is enough energy generated by the linear growth mechanism to allow the exponential growth mechanism to become large. Notably, tests with Janssen wind input, Komen wind input, and Yan wind input do not show this; only ST6 does. Therefore it is worthwhile to look in further detail. Figure 12 shows spectral output for the point indicated with a black circle in Figure 11 (*x*=88 km , *y*=52 km). Here, direction-integrated source function output are as follows: 'wind' is $S_{in,1d}(f)$, 'wcap' is $S_{wc,1d}(f)$, 'swell' is swell dissipation, $S_{swell,1d}(f)$, 'ice' is $S_{ice,1d}(f)$, 'nl4' is $S_{nl4,1d}(f)$, and 'sum5' is the sum of the five source terms just mentioned. For a uniform case and/or a case with advection disabled, 'sum5' would be equal to the growth rate. The figure indicates non-zero $S_{wc,1d}(f)$, which is not expected, from visual observations discussed in Section 3.3.3. In other words, we believe that it is probably non-physical. This provides indirect support for scaling of wind input ($\Omega_{iw} < 1$), at least for high frequency waves, and in cases where ST6 and this formula of S_{ice} is used.

The fourth and last case has all effects of the ice disabled: Figure 13. This one is even more obviously non-physical than the second and third, but again is included to verify user controls. We also confirmed (not shown) that results match a case without ice using both 41.20AB and 41.20ABi. This check was also performed with the Komen, Janssen, and Yan modes of wind input.

Based on these results we can say that of these four examples, the results with default Ω_{iw} and S_{ice} enabled are most credible. This is expected.
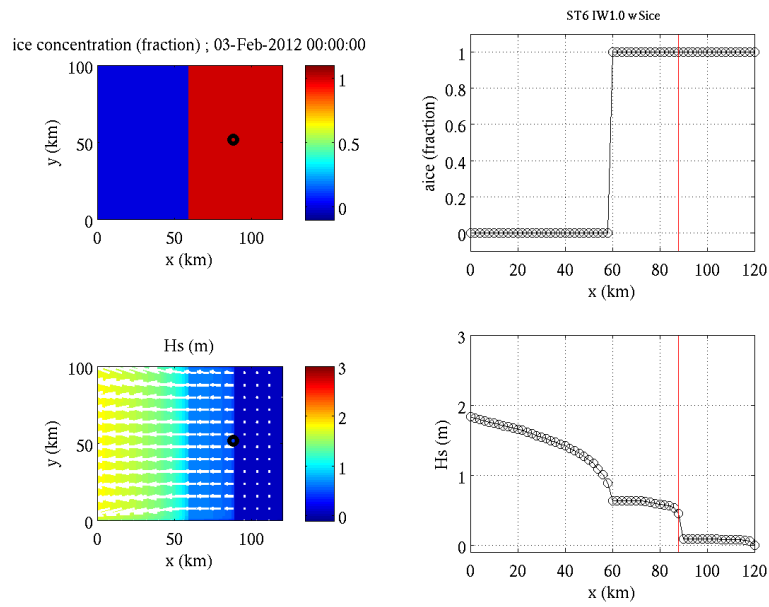
18

Figure 11. Like Figure 9, except the non-default treatment of wind input is used (ICEWIND=1), which allows wind input with 100% ice cover.
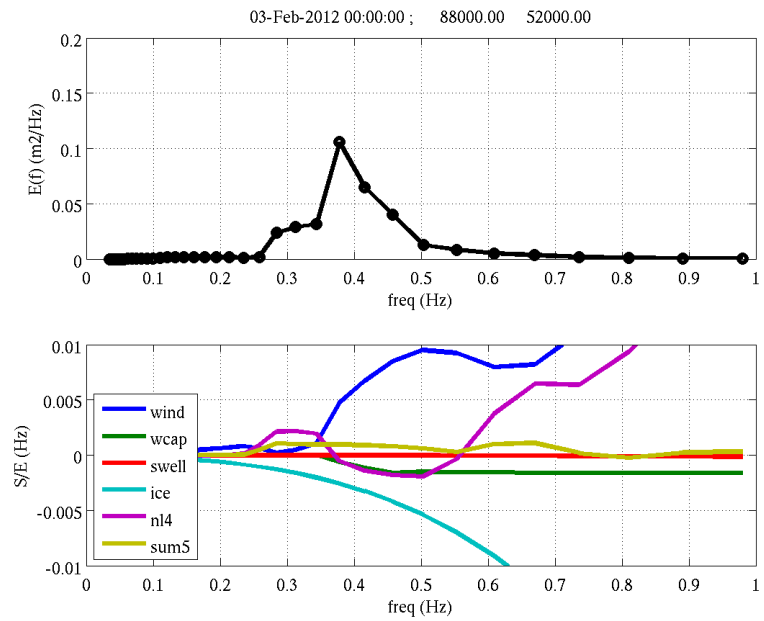

Figure 12. Spectral output from case shown in Figure 11. Upper panel: spectral density. Lower panel: source functions (see text).
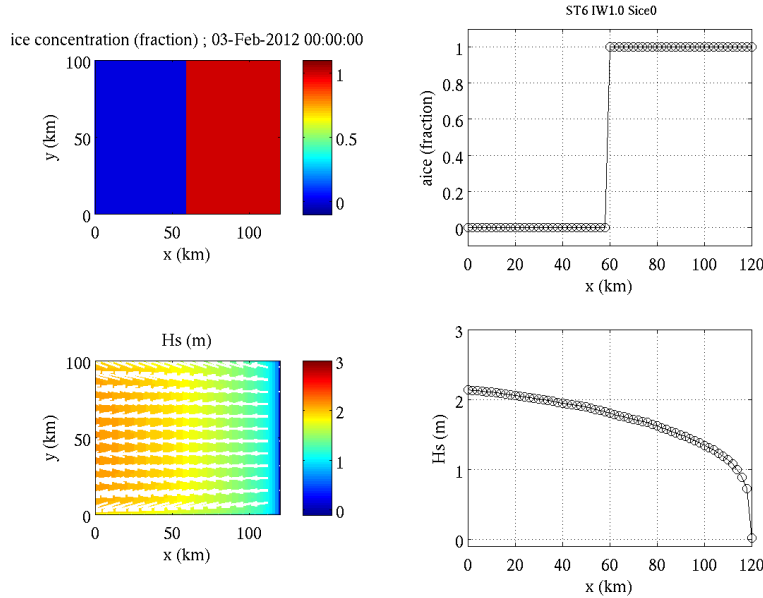
19

Figure 13. Like Figure 9, except the non-default treatment of wind input is used (ICEWIND=1) and S_{ice}=0.

5. Discussion

5.1. Discussion: Future work

We identify two "next steps" for improving the code and one additional item for future work:

1) Dissipation method using step functions. In the WW3 method of IC4M6 (Collins and Rogers 2017), the user specifies the $k_i(f)$ profile as a step function. At time of writing, this method is used for nearly all global and high-latitude applications of WW3 by NRL, including some pre-operational realtime forecasting. IC4M6 offers flexibility to input a $k_i(f)$ profile that directly uses values from a model-data inversion or comparable method. At this time, NRL is using a $k_i(f)$ profile that combines the mid-range frequency $k_i(f)$ values of Rogers et al. (2016, 2018a) and Collins and Rogers (2017) with the low-frequency $k_i(f)$ values of Ardhuin et al. (2016). The IC4M6 method is less concise than IC4M2: it requires specification of 20 numbers; WW3 uses namelist input to accomplish this.

2) Dissipation methods using h_{ice}. After ice concentration, the ice thickness is the next most commonly available ice parameter for routine application. For example, h_{ice} is a standard output from CICE (Hunke et al. 2015, see glossary) and satellite-derived products are possible (e.g. using SMOS/SMAP for thin ice, see glossary). As noted in Section 3.3.1, we have already included code for reading in ice thickness in SWAN 40.21ABi, but we have not added any S_{ice} formula to use it yet. The obvious next step is to do this. There are at least two possible approaches:

   a) Complex wavenumber solvers. Methods exist in WW3 which use h_{ice}, of course, in particular the ones that modify the dispersion relation. Based on our experience with WW3, we recommend that the simpler viscosity-only method of Keller (1998) be adopted for SWAN before moving to any visco-elastic (VE) method.

   b) Extension of parametric model. In Section 3.3.2, we gave two examples for IC4M2, for two different field studies and ice types. For each field experiment, some representative ice thickness can be very roughly identified. Then, an extended IC4M2 could be created

20

which uses ice thickness as input, with scaling between these two examples. And, in principle, more than two $k_i(f)$ profiles could be used, as long as they each have a distinct associated thicknesses. Of course, this method would still suffer from the existing problem of IC4M2, which is that limited dataset(s) are applied to a general model. However, it is attractive as a method of unifying more than one dataset while also permitting a mechanism of using h_{ice}.

3) <u>Port to NRL SWAN</u>. This item is only relevant to Navy readers. The NRL SVN repository contains the SWAN code that is used operationally by the Navy. As noted in Section 3.2, we (NRL) elected to use 41.20AB as a "base" for the new code with ice, as opposed to using the trunk of the NRL SVN repository. The advantages of this were explained in in Section 3.2. However, this strategy requires NRL to port the NRL code changes (41.20AB→41.20ABi) over to the NRL SVN repository as a subsequent step. The SWAN code in the NRL SVN repository has diverged significantly from the public release version, so the NRL ice code must be ported manually. Once that is done, the new NRL ice code will be available for use by operational Navy.

5.2. Discussion: Limitations

The NRL code changes (41.20AB→41.20ABi) have the following limitations:
1) Reflection and scattering by sea ice is not represented.
2) Floe size distribution is not represented.
3) Kinematic effects—changes to phase velocity and group velocity to produce effects analogous to refraction and shoaling (respectively) by bathymetry—are not represented.
4) Nonlinear dissipation is not represented. In other words, in IC4M2, $k_i(f)$ does not depend on $E(f)$ or H_s. For example, a dissipation mechanism associated with friction at the ice-water interface would be non-linear because of the dependence on orbital velocity.
5) Ice thickness is available as an undocumented i/o feature, but it is not used for computations. It will be used in a subsequent version of SWAN (Section 5.1).
6) Nonstationary and non-uniform polynomial coefficients are not supported. In context of variable ice type ubiquitous in the real ocean, this would seem to be a useful feature. It is available as a feature in the IC4M2 of WW3. However, in WW3, it has turned out to be an impractical idea (yet to see any use) and was therefore not adopted for this initial form of IC4M2 for SWAN.
7) The ice effects have been implemented for both structured and unstructured grids. However, no testing has been performed for unstructured grids. The code is not verified for this grid type.

6. Conclusions

The NRL code changes (41.20AB→41.20ABi) to add ice i/o and ice-related source term effects to SWAN are presented and verified in this report. The verification tests produce expected behavior, and all new user controls appear to work properly.

The implemented source term for dissipation by sea ice, 'IC4M2', is a parametric/empirical approach which is fast, simple, and flexible. This makes it ideal for routine, practical application.

This verification study should, of course, be followed by validation against observational data.

21

7. Closing remarks

On the topic of dissipation by sea ice: the simplicity of the implemented S_{ice} method is, of course, also a drawback, particularly for research applications and process studies (Section 5.2). Future work may involve either an extension into one of the more academic goals, or a further development of the relatively pragmatic approach adopted so far (Section 5.1). Our aim with this initial offering is to avoid burdening the code and the user with unjustified complexity (Section 3.1). The simple method implemented here should be used as a point of reference for any new S_{ice} method. Prior to implementing any more complex method, some questions should be asked: 'Is the additional complexity supported by observational data?', 'Is there a reasonable expectation that forecast skill is improved (i.e. without a priori knowledge of wave field)?', and 'Is it impossible to recover the same behavior using the simpler method?'.

8. Glossary

3GWAM	Third Generation Wave Model
ADCIRC	The ADvanced CIR-Culation model for Shelves, Coasts and Estuaries, Luettich et al. (1992)
APL	Applied Physics Laboratory at the University of Washington
BSBT	Backward Space, Backward Time. The first order upwind implicit scheme available as an option in SWAN. It is non-default, but is commonly used.
CICE	Community Ice CodE, Hunke et al. (2015)
ECMWF	European Centre for Medium-Range Weather Forecasts, www.ecmwf.int
ECWAM	ECMWF's version of WAM. Where WAM is open source, ECWAM is not.
IC0	Designation in WW3 for the primitive treatment of ice, Tolman (2003). Ice is treated as open water, or land, as porous land (i.e. via partial blocking), depending on whether ice concentration is low, high, or intermediate (respectively).
IC4	Designation in WW3 for several parametric and empirical representations of dissipation of wave energy by sea ice using a source term, Collins and Rogers (2017).
IC1, IC2, IC3, IC5	Other treatments of dissipation by sea ice in WW3
IC4M1, IC4M2, etc.	Subset treatments within IC4 in WW3. See Collins and Rogers (2017) and Rogers et al. (2018a).
M14	Meylan et al. (2014)
NRL	Naval Research Laboratory. A detachment of NRL at Stennis Space Center, Mississippi includes the Oceanography Division.
SMOS	Soil Moisture and Ocean Salinity, a satellite with some capability to measure ice thickness in cases of thin ice using a passive radiometer.
SMAP	Soil Moisture Active Passive. A later satellite with some capability to measure ice thickness in cases of thin ice using a passive radiometer. The active component failed, so it is an unintentional misnomer. It has improved noise mitigation relative to SMOS.
ST6	Source Term Package number 6, available in SWAN (Rogers et al. 2012) and in WW3 (Zieger et al. 2015, Liu et al. 2019)
STEL	The higher order scheme of Stelling and Leendertse (1992), the default option in SWAN, implemented by Rogers et al. (2002).
SVN	Subversion, software for version control.
SWAN	Simulating WAves Nearshore, Booij et al. (1999).
UW	University of Washington.
WA3	Wave Array #3 of the Sea State field experiment, 10-14 October 2015, described in Thomson (2015), Wadhams and Thomson (2015), and Rogers et al. (2016)
WAM	WAve Model, WAMDIG (1988). The original "third generation" wave model which is distinguished from earlier models by the fact that it does not make a priori assumptions about spectral shape, but instead relies on source terms as the primary control on spectral shape.

WAVEWATCH III	According to Alves and Banner (2003), the acronym was something like "WAVE height, WATer depth, and Current Hindcasting". If true, this usage is deprecated.
WW3	WAVEWATCH III®
WW3DG	WAVEWATCH III Development Group

References

Alves, J. H. G. M., and M. L. Banner, 2003: Performance of a saturation-based dissipation-rate source term in modeling the fetch-limited evolution of wind waves. *J. Phys. Oceanogr.*, **33**, 1274-1298.

Ardhuin, F., P. Sutherland, M. Doble, and P. Wadhams (2016). Ocean waves across the Arctic: Attenuation due to dissipation dominates over scattering for periods longer than 19 s, *Geophys. Res. Lett.,* **43**, 5775–5783, doi:10.1002/2016GL068204.

Asher, T. (2012). Addition of ice into wave predictions in the coupled ADCIRC-SWAN model, a presentation at the April 24 2012 ADCIRC Workshop, 13 slides.

Booij, N., R. C. Ris, and L. H. Holthuijsen (1999). A third-generation wave model for coastal regions, Part 1: Model description and validation. *J. Geophys. Res.,* **104** (C4), 7649-7666.

Cavaleri, L. and P. Malanotte-Rizzoli (1981). Wind wave prediction in shallow water: theory and applications. *J. Geophys. Res.,* **86**, 10961–10975.

Collins, C.O., and W.E. Rogers (2017). A Source Term for Wave Attenuation by Sea ice in WAVEWATCH III®: IC4, NRL Report NRL/MR/7320--17-9726, 25 pp. [available from www7320.nrlssc.navy.mil/pubs.php].

Doble, M. J., and J.-R. Bidlot (2013). Wavebuoy measurements at the Antarctic sea ice edge compared with an enhanced ECMWF WAM: progress towards global waves-in-ice modeling, *Ocean Model.,* **70**, 166–173, doi:10.1016/j.ocemod.2013.05.012.

Donelan, M.A., A.V. Babanin, I.R. Young, M.L. Banner (2006). Wave follower field measurements of the wind input spectral function. Part II. Parameterization of the wind input. *J. Phys. Oceanogr.,* **36**, 1672–1688.

Hunke, E. C., W. H. Lipscomb, A.K. Turner, N. Jeffery, and S. Elliot (2015). *CICE: The Los Alamos Sea Ice Model. Documentation and Software User's Manual. Version 5.1*. Los Alamos National Laboratory, Tech. Rep. LA-CC-06-012, 116 pp.

Janssen, P.A.E.M. (1989). Wave-induced stress and the drag of air flow over sea waves. *J. Phys. Oceanogr.* **19**, 745-754.

Janssen, P.A.E.M. (1991). Quasi-linear theory of wind-wave generation applied to wave forecasting. *J. Phys. Oceanogr.,* **21**, 1631–1642.

Keller, J.B. (1998). Gravity waves on ice-covered water. *J. Geophy. Res.*, **103** (C4): 7663-7669.

Komen, G. J., S. Hasselmann, and K. Hasselmann (1984). On the existence of a fully developed wind-sea spectrum. *J. Phys. Oceanogr.,* **14**, 1271-1285.

Komen, G. J., L. Cavaleri, M. Donelan, K. Hasselmann, S. Hasselmann, and P. A. E. M. Janssen (1994). *Dynamics and Modelling of Ocean Waves.* Cambridge Univ. Press, 532 pp.

Liu, Q., W. E. Rogers, A. V. Babanin, I. R. Young, L. Romero, S. Zieger, F. Qiao, C. Guan (2019). Observation-based source terms in the third-generation wave model WAVEWATCH III: updates and verification, *J. Phys. Oceanogr*. **49**. 489-517.

Luettich, R.A., Westerink, J.J., Scheffner, N.W. (1992). ADCIRC: An advanced three-dimensional circulation model for shelves, coasts, and estuaries. Report 1: Theory and methodology of ADCIRC-2DDI and ADCIRC-3DL. Technical Report DRP-92-6, USAE, Vicksburg, MS, 137 pp.

Meylan, M., L. G. Bennetts, and A. L. Kohout (2014). In situ measurements and analysis of ocean waves in the Antarctic marginal ice zone, *Geophys. Res. Lett.*, **41**, 5046–5051, doi:10.1002/2014GL060809.

Rogers, W. E. and M. D. Orzech (2013). Implementation and testing of ice and mud source functions in WAVEWATCH III®. NRL Memorandum Report, NRL/MR/7320-13-9462, 31pp. [available from www7320.nrlssc.navy.mil/pubs.php].

Rogers, W. E., J. M. Kaihatu, N. Booij, L. H. Holthuijsen, and H. Petit (2002). "Diffusion Reduction in an Arbitrary Scale Wave Action Model", *Ocean Eng*, **29**, 1357-1390.

Rogers, W. E., A. V. Babanin, and D. W. Wang (2012). Observation-Consistent Input and Whitecapping Dissipation in a Model for Wind-Generated Surface Waves: Description and Simple Calculations. *J. Atmos. Oceanic Tech., ***29***(9), 1329-1346*.

Rogers, W.E., J. Thomson, H.H. Shen, M.J. Doble, P. Wadhams and S. Cheng (2016). Dissipation of wind waves by pancake and frazil ice in the autumn Beaufort Sea, *J. Geophys. Res.*, **121,** 7991-8007, doi:10.1002/2016JC012251.

Rogers, W.E., P. Posey, L. Li, R. A. Allard (2018a). Forecasting and hindcasting waves in and near the marginal ice zone: Wave modeling and the ONR "Sea State" field experiment. *NRL Report NRL/MR/7320--18-9786,* 179 pp. [available from www7320.nrlssc.navy.mil/pubs.php].

Rogers, W.E., M.H. Meylan, A.L. Kohout (2018b). Frequency distribution of dissipation of energy of ocean waves by sea ice using data from Wave Array 3 of the ONR "Sea State" field experiment. *NRL Report NRL/MR/7322--18-9801*, 25 pp. [available from www7320.nrlssc.navy.mil/pubs.php].

Snyder, R.L., F.W. Dobson, J.A. Elliot, and R.B. Long (1981). A field study of wind generation of ocean waves. *J. Fluid Mech.*, **102**, 1–59.

Stelling, G. S., and J. J. Leendertse (1992). Approximation of convective processes by cyclic AOI methods. *Proceedings, 2nd International Conference on Estuarine and Coastal Modeling*, Tampa, Florida, ASCE, 771-782.

SWAN team (2018). SWAN User Manual, SWAN Cycle III version 41.20AB, Delft University of Technology, http://www.swan.tudelft.nl, 133 pp.

Thomson, J. (2015). ONR Sea State DRI Cruise Report: R/V Sikuliaq, Fall 2015 (SKQ201512S), retrieved from http://www.apl.washington.edu/project/project.php?id=arctic_sea_state on Mar. 14 2019. 45 pp.

Tolman, H. L. (1991). A Third-generation model for wind-waves on slowly varying, unsteady, and inhomogeneous depths and currents, *J. Phys. Oceanogr.* **21**(6*),* 782-797.

Tolman, H. L. (1992). Effects of numerics on the physics in a third-generation wind-wave model. *J. Phys. Oceanogr.*, **22**, 1095-1111.

Tolman, H. L. (1997). *User manual and system documentation of WAVEWATCH-III version 1.15*, Tech. Note 151 NOAA/NWS/NCEP/MMAB, 104 pp.

Tolman, H. L. (2002). *User manual and system documentation of WAVEWATCH-III version 2.22*, Tech. Note 222, NOAA/NWS/NCEP/MMAB, 133 pp.

Tolman, H. L. (2003). Treatment of unresolved islands and ice in wind wave models, *Ocean Modelling, 5*, 219-231.

Tolman, H. L. and the WAVEWATCH III® Development Group (2014). *User Manual and System Documentation of WAVEWATCH III® version 4.18*, *Tech. Note 316, NOAA/NWS/NCEP/MMAB*, 282 pp. + Appendices.

Tsagareli, K.N., A.V. Babanin, D.J. Walker, and I.R. Young (2010). Numerical investigation of spectral evolution of wind waves. Part 1. Wind input source function. *J. Phys. Oceanogr.,* **40**, 656-666.

Tuomi, L., K.K. Kahma, and H. Pettersson (2011). Wave hindcast statistics in the seasonally ice-covered Baltic Sea, Boreal Env. Res., 16, 451-472.

van der Westhuysen, A.J., Zijlema, M., Battjes, J.A. (2007). Nonlinear saturation-based whitecapping dissipation in SWAN for deep and shallow water. *Coastal Eng.* **54**(2), 151-170.

Wadhams, P. and J. Thomson (2015). The Arctic Ocean cruise of R/V Sikuliaq 2015, An investigation of waves and the advancing ice edge. *Il Polo,* **LXX-4,** 9-38.

WAMDI Group (1988). The WAM model--A third generation ocean wave prediction model. *J. Phys. Oceanogr.,* **18***,* 1775-1810.

WAVEWATCH III® Development Group (WW3DG) (2016). User manual and system documentation of WAVEWATCH III® version 5.16. Tech. Note 329, NOAA/NWS/NCEP/MMAB, College Park, MD, USA, 326 pp. + Appendices.

Zieger, S., A. V. Babanin, W. E. Rogers and I. R. Young (2015). Observation-based source terms in the third-generation wave model WAVEWATCH. *Ocean Modelling*, **96**, doi:10.1016/j.ocemod.2015.07.014